Journal of Sound and Vibration (2000) **230**(1), 171–185
doi:10.1006/jsvi.1999.2608, available online at http://www.idealibrary.com on IDEAL®

EFFECT OF FLUID DEPTH ON THE HYDROELASTIC VIBRATION OF FREE-EDGE CIRCULAR PLATE

M. K. KWAK

Department of Mechanical Engineering, Dongguk University, 26 Pil-Dong 3-Ga, Joong-Gu, Seoul 100-715, Korea

AND

S.-B. HAN

Department of Mechanical Design, Kyungnam University, #449, Wolyoung-Dong, Habpo-Gu, Masan, Kyungnam 631-701, Korea

(*Received* 3 *February* 1999, *and in final form* 27 *August* 1999)

This paper is concerned with the effect of water depth on the free vibration of free-edge circular plates resting on a free fluid surface. The problem addressed is formulated by using the Hankel transformation method, which leads to dual integral equations. The solution of dual integral equations is solved numerically by using Fourier–Bessel series. The fluid is assumed to be inviscid and incompressible. The Kirchhoff theory of plates is used to model the elastic thin plate. Numerical results are given in non-dimensional form for free-edge circular plates, in order to be ready-to-use in applications. To validate the theoretical results, experiments were carried out. Experimental results are in good agreement with theoretical results. It is found that the effect of the fluid depth can be neglected when the fluid depth is greater than the diameter of the circular plates but becomes significant as the water depth decreases. It is also observed in the experimental results that the fluid damping increases as the water depth decreases.

1. INTRODUCTION

There have been many studies concerning vibrations of circular plates in contact with fluid. After the pioneering work of Lord Rayleigh [1], the first study on this topic can be attributed to Lamb [2]. He studied the free vibrations of clamped, circular baffled plates by using simple assumed modes and an approximation to obtain the hydrodynamic pressure; this solution was extended to free-edge circular plates by McLachlan [3]. Amabili and Kwak [4] have recently solved the same problem by using a refined approach and Kwak [5] obtained the solution using the Fourier–Bessel series approach.

Free vibrations of circular plates resting on a free liquid surface have been studied for the first time a few years ago by Kwak and Kim [6] for axisymmetric modes and by Kwak [7] for the general case. These studies also address circular

0022-460X/00/060171 + 15 $35.00/0

plates completely submerged in an infinite fluid domain. Experiments confirming the results of references [6, 7] have been performed by Amabili *et al.* [8]. Kwak and Amabili [9] extended this study to annular plates, successfully comparing theoretical and experimental results. In all these studies, the boundary conditions on the fluid domain are mixed and give a Dirichelet problem. In particular, a zero velocity potential is imposed at the free liquid surface, so that the effect of free surface waves is neglected.

Other interesting studies on vibrations of circular plates in stationary fluids can be found in the literature, e.g., references [10–14].

The present study addresses itself to free vibrations of circular plates resting on a free fluid surface, which is the same problem already solved by Kwak [7]; however, in this study the effect of water depth is included. Amabili [15] investigated theoretically the effect of fluid depth on the vibration of baffled circular plates. Amabili [15] dealt with two cases; the baffled circular plate is located at the bottom and it is limited by the rigid upper plane and the baffled circular plate is located at the bottom and the upper plane is replaced by the free surface. The problem considered in this paper is different from the cases considered by Amabili [15] in which circular plate is put on the free surface and the fluid is limited by the rigid bottom. The reason for choosing this problem is that this case can be easily dealt with experimentally. In addition, the free surface condition results in the mixed boundary value problem [16].

The fluid is assumed to be inviscid and incompressible so that the fluid motion can be described by the velocity potential. The Kirchhoff theory of plates [17] is used to model the elastic thin plate. Unfortunately, the closed-form solution cannot be derived in this case. Hence, we resort to the numerical method to obtain the non-dimensional parameters. Numerical results are then compared with the experimental results. The experimental results are in good agreement with the theoretical results and show that natural frequencies decreases rapidly as the water depth becomes very shallow. However, the effect of water depth can be neglected if the water depth is larger than the diameter of the circular plates. In this case, we can use the results obtained by Kwak and Kim [6] and Kwak [7].

2. MIXED BOUNDARY VALUE PROBLEM

Let us consider a circular plate and a polar co-ordinate system (O, r, θ) with the pole O at the centre of the plate as shown in Figure 1. The transverse deflection w for *in vacuo* free vibrations of thin elastic circular plates is generally expressed by

$$w(r, \theta, t) = W_{nm}(r)\cos(n\theta)\sin(\omega t), \tag{1}$$

where $W_{nm}(r) = [\mathrm{J}_n(\lambda_{nm}r/a) + \alpha_{nm}\mathrm{I}_n(\lambda_{nm}r/a)]$ represents the mode shape, n is the number of nodal diameters, m is the number of nodal circles, ω is the radian frequency, and λ_{nm} and α_{nm} are the frequency and mode-shape parameters, respectively, both depending on the plate's boundary conditions. J_n and I_n indicate the Bessel function and the modified Bessel function of order n respectively. The

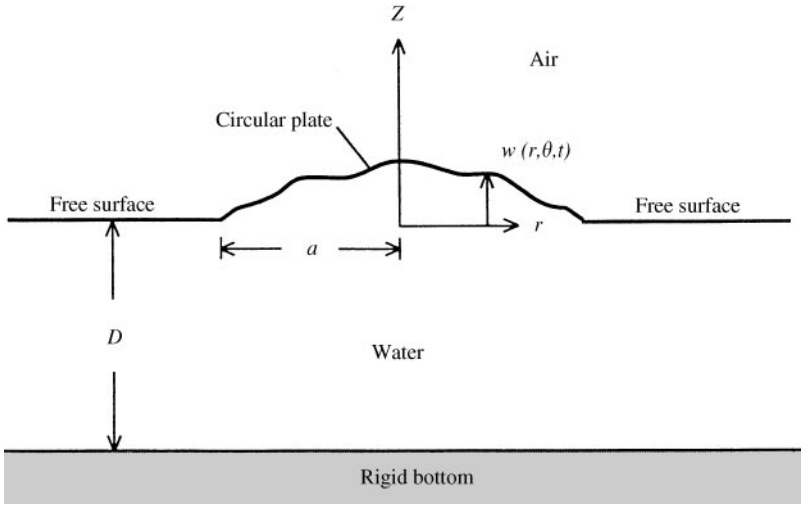

Figure 1. Circular plate on a free fluid surface; co-ordinate system and symbols.

equations for λ_{nm} and α_{nm} are given in section 2; some of these data can be found in reference [18]. The radian *in vacuo* frequency of vibration ω_V and the frequency parameter λ_{nm} are related by

$$\omega_V = \lambda_{nm}^2 \sqrt{D/(\rho_P h a^4)}, \tag{2}$$

where $D = (Eh^3)/[12(1 - v^2)]$, ρ_P is the plate mass density, h is the plate thickness, a is the plate radius, E is Young's modulus and v is the Poisson ratio. In deriving equation (2), the Kirchhoff theory of plates [17] was used.

Let us introduce the hypothesis that the mode-shapes of a vibrating plate on a fluid surface are the same as *in vacuo*. This amounts to saying that the dynamic loading of the fluid is assumed to have a negligible effect on the natural mode shapes of the plate. Experimental tests, performed by Montero de Espinosa and Gallego-Juàrez [10], Amabili *et al.* [8] and Amabili and Kwak [9] show that mode shapes are little modified by the presence of water, especially for free-edge plates. Amabili and Kwak [4] theoretically computed the actual mode shapes of a baffled circular plate in contact with liquid on one side. They have shown that the actual mode shapes are quite close to the ones *in vacuo*, and for free-edge plates the differences are particularly small. With this assumption, equation (1) is also valid for a plate on the fluid surface.

If the fluid is incompressible and inviscid and its movement is irrotational, it is possible to describe the fluid motion (due to the plate's vibration) by means of the velocity potential Φ, which satisfies the Laplace equation $\nabla^2\Phi = 0$. Then, the fluid velocity is given by $\mathbf{v} = -\nabla\Phi$. By using the separation of variables with respect to the cylindrical co-ordinate, Φ can be expressed as

$$\Phi(r, \theta, z, t) = \phi(r, z)\cos(n\theta)\,\omega\cos(\omega t), \tag{3}$$

where ω is the radian frequency of the fluid–plate system and ϕ satisfies

$$\frac{\partial^2\phi}{\partial r^2} + \frac{\partial\phi}{r\partial r} + \frac{\partial\phi}{\partial z^2} - \frac{n^2}{r^2}\phi = 0 \quad \text{in the fluid domain.} \tag{4}$$

Based on the problem considered in this paper, the following conditions are imposed: (1) a contact without cavitation at the fluid–plate interface S_B and the fluid–bottom interface, S_D; (2) the linearized free surface condition on the free fluid surface S_F and (3) the radiation condition at an infinite distance from the plate S_R (see Figure 1). The superficial tension of the fluid is neglected. Therefore, the boundary conditions can be expressed as

$$\frac{\partial\phi}{\partial z} = -W_{mn}(r) \quad \text{on } S_B, \tag{5}$$

$$\phi = 0 \quad \text{on } S_F, \tag{6}$$

$$\phi, \frac{\partial\phi}{\partial r} \to 0 \quad \text{on } S_R, \tag{7}$$

$$\frac{\partial\phi}{\partial z} = 0 \quad \text{on } S_D. \tag{8}$$

In order to solve the mixed boundary value problem it is useful to use the modified Hankel transformation, as addressed by Kwak and Kim [6] and Kwak [7]. It is defined as

$$\overline{\phi_h} = \int_0^\infty r\phi(r, z)\mathrm{J}_n(\xi r)\,\mathrm{d}r. \tag{9}$$

Using equation (9), equation (4) can be reduced to the following ordinary differential equation:

$$\frac{\mathrm{d}^2\overline{\phi_h}}{\mathrm{d}z^2} - \xi^2\overline{\phi_h} = 0. \tag{10}$$

The general solution of equation (10) is

$$\overline{\phi_h}(\xi, z) = A(a\xi)\mathrm{e}^{\xi z} + B(a\xi)\mathrm{e}^{-\xi z} \tag{11}$$

Inserting equation (11) into the boundary condition, equation (8), we obtain

$$A(a\xi) = B(a\xi)\mathrm{e}^{2\xi D}. \tag{12}$$

Hence, equation (11) can be rewritten as

$$\overline{\phi_h}(\xi, z) = B(a\xi)(\mathrm{e}^{2\xi D}\mathrm{e}^{\xi z} + \mathrm{e}^{-\xi z}). \tag{13}$$

The inversion formula for the Hankel transform gives

$$\phi(r, z) = \int_0^\infty \xi\overline{\phi_h}(\xi, z)\mathrm{J}_n(\xi r)\,\mathrm{d}\xi. \tag{14}$$

Using equations (5), (6) and (14), the mixed boundary value problem for the addressed problem can be represented by the following dual integral equation:

$$\begin{gathered}\int_0^\infty \xi^2 B(a\xi)(\mathrm{e}^{2\xi D} - 1)\mathrm{J}_n(\xi r) = -W_{nm}(r), \quad 0 < r \leqslant a,\\ \int_0^\infty \xi B(a\xi)(\mathrm{e}^{2\xi D} + 1)\mathrm{J}_n(\xi r) = 0, \quad r > a,\end{gathered} \tag{15}$$

Let us introduce the following non-dimensional variables to simplify the formulation

$$\rho = \frac{r}{a}, \qquad \eta = a\xi, \qquad \delta = \frac{D}{a}, \qquad A(\eta) = \eta^2 B(\eta)(\mathrm{e}^{2\delta\eta} + 1). \tag{16}$$

Then, the transformed dual integral equations become

$$\begin{gathered}\int_0^\infty \tanh\delta\eta A(\eta)\mathrm{J}_n(\rho\eta)\,\mathrm{d}\eta = a^3 W_{nm}(\rho), \quad 0 < \rho \leqslant 1,\\ \int_0^\infty \eta^{-1} A(\eta)\mathrm{J}_n(\rho\eta)\,\mathrm{d}\eta = 0, \quad \rho > 1.\end{gathered} \tag{17}$$

Let us employ the following series expansion to obtain the approximate solution of the above dual integral equation:

$$A(\eta) = a^3 \sum_{j=0}^{\infty} c_j \mathrm{J}_{n+2f+2}(\eta). \tag{18}$$

We also use the following property of the Bessel function [19]:

$$\int_0^\infty x^{-1}\mathrm{J}_{n+2i+2}(\alpha x)\mathrm{J}_n(\beta x)\,\mathrm{d}x = 0, \quad \text{for } \beta > \alpha, \tag{19}$$

Therefore, the second equation of equation (17) is automatically satisfied. Inserting equation (18) into the first equation of equation (17) results in

$$\sum_{j=0}^{\infty} c_j \int_0^{\infty} \tanh \delta\eta \mathrm{J}_{n+2j+2}(\eta)\mathrm{J}_n(\rho\eta)\,\mathrm{d}\eta = W_{nm}(\rho). \tag{20}$$

We will use the following integral formula to solve the above equation:

$$\eta^{-2}\mathrm{J}_{n+2i+2}(\eta) = \frac{\Gamma(1+n+i)}{2\Gamma(2+i)\Gamma(1+n)}$$

$$\int_0^1 \rho^{n+1}\,{}_2\mathrm{F}_1(1+n+i,\ -1-i,\ 1+n,\ \rho^2)\mathrm{J}_n(\rho\eta)\,\mathrm{d}\rho, \tag{21}$$

where Γ is the Gamma function and ${}_2\mathrm{F}_1$ is the hypergeometric function respectively.

Hence, equation (20) can be expressed as

$$\sum_{i=0}^{\infty} K_{ij}c_j = b_i \quad \text{for } i = 0, 1, 2, \ldots, \infty, \tag{22}$$

where

$$K_{ij} = \int_0^{\infty} \eta^{-2} \tanh \delta\eta \mathrm{J}_{n+2i+2}(\eta)\mathrm{J}_{n+2j+2}(\eta)\,\mathrm{d}\eta, \tag{23a}$$

$$b_i = \frac{\Gamma(1+n+i)}{2\Gamma(2+i)\Gamma(1+n)} \int_0^1 \rho^{n+1} W_{nm}(\rho)\,{}_2\mathrm{F}_1(1+n+i,\ -1-i,\ 1+n,\ \rho^2)\,\mathrm{d}\rho. \tag{23b}$$

By solving the simultaneous equation (22), the coefficient of series c_j can be obtained. The numerical calculation was carried out using Mathematica [20].

3. NON-DIMENSIONAL ADDED VIRTUAL MASS INCREMENTAL FACTOR

In section 2 it is assumed that the wet mode shapes are the same as the mode shapes *in vacuo*, so that there is no change in kinetic and elastic potential energies of the plate. For a plate vibrating *in vacuo* one can write

$$\omega_V^2 = \frac{V_P}{T_P^*}, \tag{24}$$

where ω_V is the radian frequency of the plate *in vacuo*, V_P is the maximum potential energy of the plate and T_P^* is its reference kinetic energy. Based on the assumption that the wet mode shapes are the same as the dry mode shapes mentioned earlier, we can write

$$\omega_F^2 = \frac{V_P}{T_P^* + T_F^*}, \tag{25}$$

where ω_F is the radian frequency of the plate in contact with the fluid surface, and T_F^* is the reference kinetic energy of the fluid. Using equations (24) and (25), we can derive

$$\omega_V^2 = \left(1 + \frac{T_F^*}{T_P^*}\right)\omega_F^2. \tag{26}$$

Let us first derive the kinetic energy of the fluid. Using the non-dimensional variables, the potential at the free surface can be expressed as

$$\phi(\rho, 0) = \frac{1}{a^2}\int_0^\infty A(\eta)\mathrm{J}_n(\rho\eta)\,\mathrm{d}\eta. \tag{27}$$

Inserting equation (18) into equation (27), we obtain

$$\phi(\rho, 0) = a\sum_{i=0}^{\infty}\frac{c_i\Gamma(1+n+i)}{2\Gamma(2+i)\Gamma(1+n)}\rho^{n+1}\,{}_2\mathrm{F}_1(1+n+i,\ -1-i,\ 1+n,\ \rho^2). \tag{28}$$

It is well-known that using Green's theorem [21, 22] it is possible to evaluate the reference kinetic energy of the fluid with a surface integral on the boundary of the fluid domain. The boundary conditions, equations (6)–(8), imply that the integrals on $S_R + S_F + S_D$ are zero. Hence, the reference kinetic energy of the fluid computed by integrating only over the wet plate surface S_B, is then expressed as

$$T_F^* = -\frac{1}{2}\rho_F a^2 D_n\int_0^1 \phi(\rho, 0)\frac{\partial\phi(\rho, 0)}{\partial z}\,\mathrm{d}\rho = \frac{1}{2}\rho_F a^2 D_n\int_0^1 \phi(\rho, 0)W_{nm}(\rho)\,\mathrm{d}\rho, \tag{29}$$

where

$$D_n = \begin{cases} 2\pi & \text{if } n = 0, \\ \pi & \text{if } n \geqslant 1. \end{cases} \tag{30}$$

Inserting equation (28) into equation (29), the reference kinetic energy of the fluid is expressed as

$$T_F^* = \tfrac{1}{2}\rho_F a^3 D_n \Delta_F, \tag{31}$$

where

$$\Delta_F = \sum_{i=0}^{\infty} \frac{c_i \Gamma(1+n+i)}{2\Gamma(2+i)\Gamma(1+n)} \int_0^1 \rho^{n+1} W_{nm}(\rho)\, {}_2\mathrm{F}_1(1+n+i,\ -1-i,\ 1+n,\ \rho^2)\, \mathrm{d}\rho. \tag{32}$$

The kinetic energy of the plate can be expressed as [7]

$$T_P^* = \tfrac{1}{2} \rho_P h D_n a^2 \Delta_P, \tag{33}$$

where

$$\Delta_P = \tfrac{1}{2}[\delta_{P1} + 2\alpha_{nm}\delta_{P2} + \alpha_{nm}^2 \delta_{P3}] \tag{34}$$

in which

$$\delta_{P1} = \mathrm{J}_n^2(\lambda_{nm}) - \mathrm{J}_{n-1}(\lambda_{nm})\mathrm{J}_{n+1}(\lambda_{nm}),$$

$$\delta_{P2} = \frac{1}{\lambda_{nm}}[\mathrm{J}_n(\lambda_{nm})\mathrm{I}_{n-1}(\lambda_{nm}) - \mathrm{J}_{n-1}(\lambda_{nm})\,\mathrm{I}_n(\lambda_{nm})],$$

$$\delta_{P3} = \mathrm{I}_n^2(\lambda_{nm}) - \mathrm{I}_{n-1}(\lambda_{nm})\mathrm{I}_{n+1}(\lambda_{nm}). \tag{35}$$

Hence, the ratio of the fluid kinetic energy and the water kinetic energy can be expressed in terms of the non-dimensional parameters [7]:

$$\frac{T_F^*}{T_P^*} = \left(\frac{\rho_F a}{\rho_P h}\right)\frac{\Delta_F}{\Delta_P} = \beta \Gamma_{nm} \tag{36}$$

in which $\beta = \rho_F a/\rho_P h$ is the so-called thickness correction factor and $\Gamma_{nm} = \Delta_F/\Delta_P$ is the non-dimensionalized added virtual mass incremental (NAVMI) factor [6, 7] or zeroth order NAVMI factor. Hence, one can express the frequency change in the form

$$\frac{\omega_F}{\omega_V} = \frac{1}{\sqrt{1+\beta\Gamma_{nm}}}. \tag{37}$$

4. NUMERICAL RESULTS

The frequency and mode shape parameters for free-edge circular plates *in vacuo* have been reported in many studies including references [18, 23]. The frequency parameters of circular plates having free-edge boundary conditions can be obtained

by solving the following characteristic equations:

$$\frac{\lambda_{nm}^2 \mathrm{J}_n(\lambda_{nm}) + (1-\nu)[\lambda_{nm}\mathrm{J}'_n(\lambda_{nm}) - n^2\mathrm{J}_n(\lambda_{nm})]}{\lambda_{nm}^2 \mathrm{I}_n(\lambda_{nm}) - (1-\nu)[\lambda_{nm}\mathrm{I}'_n(\lambda_{nm}) - n^2\mathrm{I}_n(\lambda_{nm})]}$$

$$= \frac{\lambda_{nm}^2 \mathrm{J}'_n(\lambda_{nm}) + (1-\nu)n^2[\lambda_{nm}\mathrm{J}'_n(\lambda_{nm}) - \mathrm{J}_n(\lambda_{nm})]}{\lambda_{nm}^2 \mathrm{I}'_n(\lambda_{nm}) - (1-\nu)n^2[\lambda_{mn}\mathrm{I}'_n(\lambda_{nm}) - \mathrm{I}_n(\lambda_{nm})]}, \tag{38}$$

where J'_n and I'_n indicate the derivatives of Bessel functions with respect to the argument.

The mode-shape parameter for free-edge circular plates can be calculated by using the following equations:

$$\alpha_{nm} = \frac{\lambda_{nm}^2 \mathrm{J}_n(\lambda_{nm}) + (1-\nu)[\lambda_{nm}\mathrm{J}'_n(\lambda_{nm}) - n^2\mathrm{J}_n(\lambda_{nm})]}{\lambda_{nm}^2 \mathrm{I}_n(\lambda_{nm}) - (1-\nu)[\lambda_{nm}\mathrm{I}'_n(\lambda_{nm}) - n^2\mathrm{I}_n(\lambda_{nm})]}. \tag{39}$$

The various NAVMI factors Γ_{nm} with respect to the depth ratio are plotted as lines in Figures 2–6. In solving equation (22), 10 terms were used. The numerical results show that the coefficients converge to zero rapidly; hence the 10-term approximation is validated. The NAVMI factors which can be extracted from the graphs are ready-to-use in applications, in conjunction with equation (37), due to their non-dimensional form.

5. EXPERIMENTS

To verify the theoretical results, the experiments were carried out for the circular steel plate which has a 150 mm radius and a 2 mm thickness. This plate was put

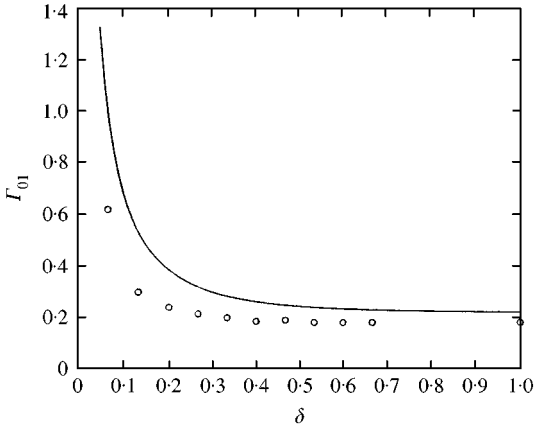

Figure 2. NAVMI factor for ($n = 0, m = 1$). —, theory; ○, experiment.

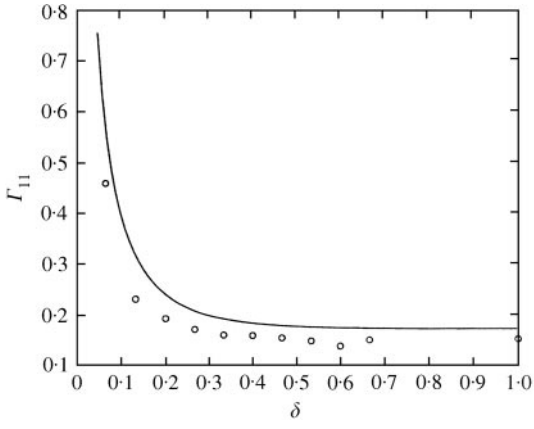

Figure 3. NAVMI factor for ($n = 1, m = 1$). —, theory; ○, experiment.

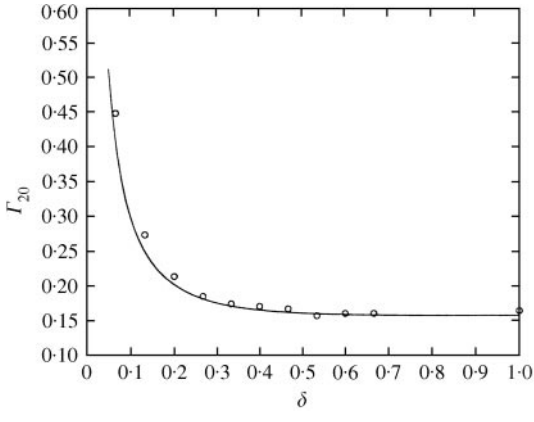

Figure 4. NAVMI factor for ($n = 2, m = 0$). —, theory; ○, experiment.

inside the water tank which was 1·5 m in height and 1·2 m in diameter, and was supported by the string thus enabling the free-edge boundary condition. The size of the circular plate was relatively small compared to the size of the cylindrical water tank, so that the wave reflected from the wall can be ignored. We immersed half of the plate's thickness in the water very carefully. The impulse hammer was used to excite the circular plate and the small accelerometer (PCB 303 A03) which weighed 1·9 g was attached to the plate. The mass ratio of the accelerometer to the mass of the plate is 2·2%. Hence, the influence of the mass increase due to the accelerometer on the natural frequencies was expected to be small. The signals from the hammer and the accelerometer were fed into the B & K 3550 FFT signal analyzer to compute the frequency response function (FRF). The frequency bandwidth was limited to 1·6 kHz.

The natural frequencies of the circular plates in air are measured and compared to the theoretical frequencies in Table 1 to confirm that the uniform and perfect

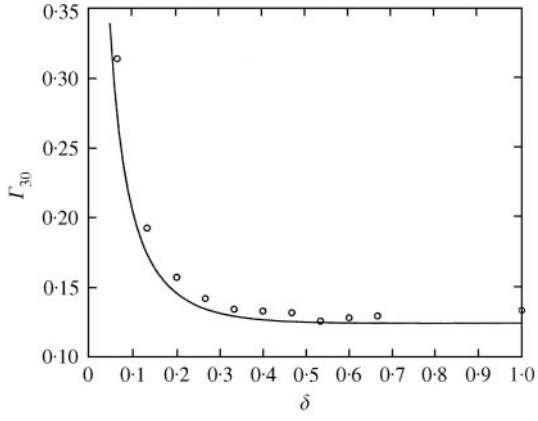

Figure 5. NAVMI factor for ($n = 3, m = 0$). —, theory; ○, experiment.

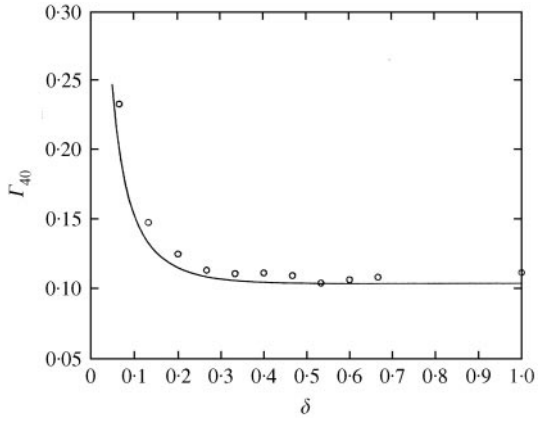

Figure 6. NAVMI factor for ($n = 4, m = 0$). —, theory; ○, experiment.

TABLE 1

The experimental and theoretical natural frequencies of the free-edge circular plate in air

(m, n)	(2, 0)	(0, 1)	(3, 0)	(1, 1)	(4, 0)
f_a (Experiment) (Hz)	127	212	288	451	501
f_a (Theory) (Hz)	123	206	285	468	499

circular plate is manufactured. The material and geometrical properties of the circular plate which is made of mild steel are $\rho_P = 7730\ \text{kg/m}^3$ and $\alpha = 0{\cdot}15\ \text{m}$, $h = 0{\cdot}002\ \text{m}$, $E = 210\ \text{GPa}$. The theoretical results are in good agreement with the experimental ones as shown in Table 1.

TABLE 2

The experimental natural frequencies of the free-edge circular plate in water versus water depth

Depth (cm) \ (*m*, *n*)	(2, 0)	(0, 1)	(3, 0)	(1, 1)	(4, 0)
1	55·5	81·0	144·5	195·0	280·0
2	67·0	108·5	171·5	252·5	323·5
3	73·0	117·5	182·5	268·0	339·0
4	76·5	122·0	188·0	278·0	348·0
5	78·0	125·0	191·0	284·0	350·0
6	78·5	128·0	191·5	284·5	349·5
7	79·0	127·0	192·0	287·0	351·0
8	80·5	129·0	194·5	290·5	355·5
9	80·0	129·0	193·5	296·5	353·5
10	80·0	129·0	193·0	289·5	352·0
15	79·5	129·0	191·5	289·0	349·5

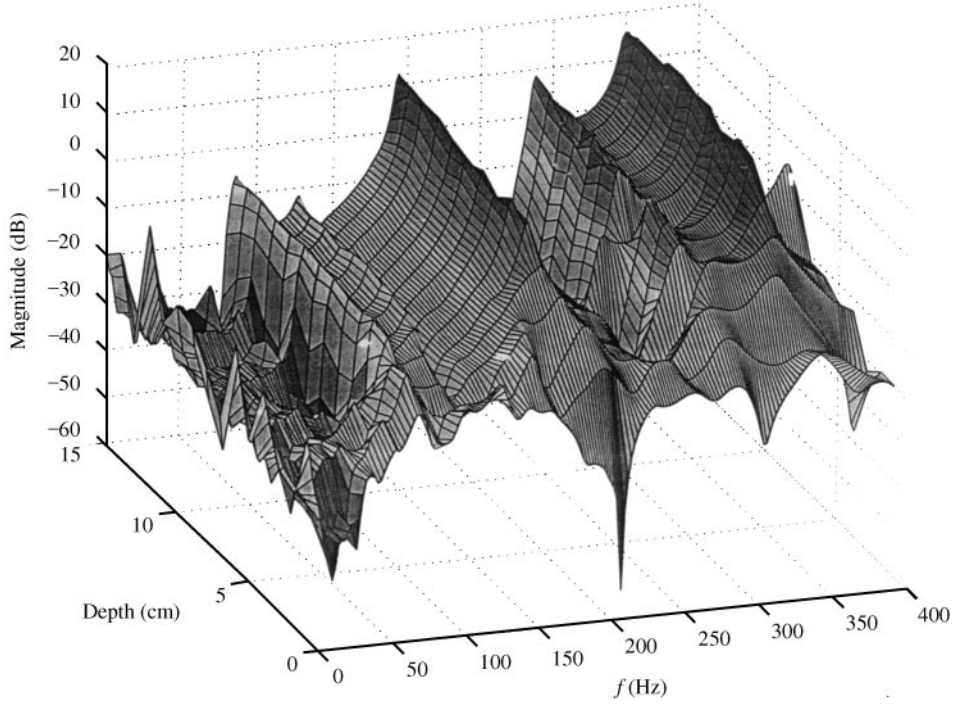

Figure 7. Frequency response functions versus depth.

The natural frequencies of the circular plate in contact with water are measured by varying the depth, which are shown in Table 2. From Tables 1 and 2, the NAVMI factors are extracted and compared to the theoretical NAVMI factors,

which are shown in Figures 2–6. As shown in Figures 2 and 3, the experimental NAVMI factors for the modes with nodal diameter are a little lower than the theoretical NAVMI factors. However, the experimental NAVMI factors for the modes without nodal diameter are in fairly good agreement with the theoretical NAVMI factors as shown in Figures 4–6. It can be said that the theoretical NAVMI factors predict the effect of water depth very well.

The natural frequencies of the plates in contact with water were extracted from the measured FRFs. Figure 7 shows the changes in the FRF in terms of water depth. As can be seen from Figure 7, when the water depth is greater than the diameter of the plate, the natural frequencies of the plate can be easily identified by the high peaks of the FRF. However, the peak values of the measured FRF decrease as the water depth decreases. Furthermore, at an extremely small value of water depth, the sharpness of the FRF shape completely disappears as shown in Figure 7. In this case, the damping value is not small and thus the natural frequencies are not identifiable with the peak points of the magnitude of the FRF. Instead, we detect the natural frequencies by checking the real and imaginary values of the FRF. The resonance region of the inertance form of the FRF is characterized by a sign change in the real part accompanied by a peak in the imaginary part.

The reason for this degeneration of the FRF shape as shown in Figure 7 is that the damping effect of the water due to the viscosity becomes significant as the water depth decreases. Theoretical derivation of the present work was based on the potential theory, in which the viscosity of the water was ignored. As revealed by the experiments, the water depth has effects not only on the virtual mass but also on the damping value of the surrounding water. This damping effect of the water depth on the natural frequencies of the plate in contact with water should be further investigated.

6. DISCUSSION AND CONCLUSIONS

In this paper, the NAVMI factors for the circular plate in contact with water including the effect of water depth are computed theoretically and compared with the experimental results. To this end, the Hankel transformation is used to simplify the boundary value problem and Fourier–Bessel series are used to solve dual integral equations. The numerical method is then employed to approximately calculate the NAVMI factors.

It is found from both theoretical and experimental results that the effect of water depth on the natural frequencies of the circular plate in contact with water becomes significant as the water depth decreases. The numerical and experimental results show that NAVMI factors increase rapidly as the water depth becomes shallow. It is found that the theoretical NAVMI factors are in good agreement with the experimental ones. However, the theoretical NAVMI factors deviate slightly from the experimental NAVMI factors as the water becomes shallow. It is also observed in experiments that the fluid damping increases as the water becomes shallow so that the estimation of natural frequencies based on the peaks of the frequency response curve becomes a difficult task.

It can be concluded that the formula and NAVMI factors derived in this study can accurately predict the changes in natural frequencies of the circular plates in contact with water including the effect of water depth. However, the fluid–structure interaction problem including fluid damping needs to be investigated.

ACKNOWLEDGMENTS

This work is supported by the research grant of Dongguk University.

REFERENCES

1. J. W. S. Lord Rayleigh 1945 *Theory of Sound*, New York: Dover, second edition (first edition, 1877).
2. H. Lamb 1921 *Proceedings of the Royal Society* (*London*) **A98**, 205–216. On the vibrations of an elastic plate in contact with water.
3. N. W. McLachlan 1932 *Proceedings of the Physical Society* (*London*) **44**, 546–555. The accession to inertia of flexible discs vibrating in a fluid.
4. M. Amabili and M. K. Kwak 1996 *Journal of Fluids and Structures* **10**, 743–761. Free vibration of circular plates coupled with liquids: revising the Lamb problem.
5. M. K. Kwak 1997 *Journal of Sound and Vibration* **201**, 293–303. Hydroelastic vibration of circular plates.
6. M. K. Kwak and K. C. Kim 1991 *Journal of Sound and Vibration* **146**, 381–389. Axisymmetric vibration of circular plates in contact with fluid.
7. M. K. Kwak 1991 *Transactions of the ASME*, *Journal of Applied Mechanics* **58**, 480–483. Vibration of circular plates in contact with water.
8. M. Amabili, G. Dalpiaz and C. Santolini 1995 *Modal Analysis*: *The International Journal of Analytical and Experimental Modal Analysis* **10**, 187–202. Free-edge circular plates vibrating in water.
9. M. K. Kwak and M. Amabili 1998 *Transactions of the ASME*, *Journal of Vibration and Acoustics* **121**, 26–32. Hydroelastic vibration of free-edge annular plates.
10. F. M. Espinosa and A. G. Gallego-Juárez 1984 *Journal of Sound and Vibration* **94**, 217–222. On the resonance frequencies of water-loaded circular plates.
11. K. Nagaia and J. Takeuchi 1984 *Journal of the Acoustical Society of America* **75**, 1511–1518. Vibration of a plate with arbitrary shape in contact with a fluid.
12. K. Nagaia and K. Nagai 1986 *Journal of Sound and Vibration* **70**, 333–345. Dynamic response of circular plates in contact with a fluid subjected to general dynamic pressures on a fluid surface.
13. J. H. Ginsberg and P. Chu 1992 *Journal of the Acoustical Society of America* **91**, 894–906. Asymmetric vibration of a heavily fluid-loaded circular plate using variational principles.
14. M. K. Kwak 1994 *Journal of Sound and Vibration* **178**, 688–690. Vibration of circular membranes in contact with fluid.
15. M. Amabili 1996 *Journal of Sound and Vibration* **193**, 909–925. Effect of finite fluid depth on the hydroelastic vibrations of circular and annular plates.
16. I. N. Sneddon 1966 *Mixed Boundary-Value Problems in Potential Theory*. Amsterdam: North-Holland.
17. G. Kirchhoff 1850 *Mathematical Journal* (*Crelle's Journal*) **40**, 51–58. Über das Gleichgewicht und die Bewegung einer elastischen Scheibe.
18. M. Amabili, A. Pasqualini and G. Dalpiaz 1995 *Journal of Sound and Vibration* **188**, 685–699. Natural frequencies and modes of free-edge circular plates vibrating in vacuum or in contact with liquid.

19. I. S. Gradshteyn and I. M. Ryzhik 1994 *Table of Integrals, Series and Products*. London: Academic Press, fifth edition.
20. S. Wolfram 1996 *The Mathematica Book*. Cambridge, U.K.: Cambridge University Press, third edition.
21. M. Amabili 1997 *Journal of Fluids and Structures* **11**, 507–523. Ritz method and substructuring in the study of vibration with strong fluid–structure interaction.
22. H. Lamb 1945 *Hydrodynamics*, 46. New York: Dover.
23. A. W. Leissa 1969 *Vibration of Plates*, NASA SP-160.